

# Robust Regularity in $\gamma$ -Soft Nuclei and its Microscopic Realization

K. Nomura,<sup>1</sup> N. Shimizu,<sup>2</sup> D. Vretenar,<sup>3</sup> T. Nikšić,<sup>3</sup> and T. Otsuka<sup>1,2,4</sup>

<sup>1</sup>*Department of physics, University of Tokyo, Hongo, Bunkyo-ku, Tokyo 113-0033, Japan*

<sup>2</sup>*Center for Nuclear Study, University of Tokyo, Hongo, Bunkyo-ku, Tokyo 113-0033, Japan*

<sup>3</sup>*Physics Department, Faculty of Science, University of Zagreb, 10000 Zagreb, Croatia*

<sup>4</sup>*National Superconducting Cyclotron Laboratory, Michigan State University, East Lansing, Michigan 48824-1321, USA*

(Dated: March 6, 2022)

$\gamma$ -softness in atomic nuclei is investigated in the framework of energy density functionals. By mapping constrained microscopic energy surfaces for a set of representative non-axial medium-heavy and heavy nuclei to a Hamiltonian of the proton-neutron interacting boson model (IBM-2) containing up to three-body interactions, low-lying collective spectra and transition rates are calculated. Observables are analyzed that distinguish between the two limiting geometrical pictures of non-axial nuclei: the rigid-triaxial rotor and the  $\gamma$ -unstable rotor. It is shown that neither of these pictures is realized in actual nuclei, and that a microscopic description leads to results that are almost exactly in between the two geometrical limits. This finding points to the optimal choice of the IBM Hamiltonian for  $\gamma$ -soft nuclei.

PACS numbers: 21.10.Re, 21.60.Ev, 21.60.Fw, 21.60.Jz

Like many other quantum systems, atomic nuclei display a variety of geometrical shapes that reflect deformations of the nuclear surface arising from collective motion of many nucleons [1]. Shapes of most non-spherical nuclei are characterized by axially-symmetric quadrupole deformations – prolate or oblate ellipsoids. There are, however, many nuclei in which axial symmetry, i.e., the invariance under rotation around the symmetry axis of the intrinsic state, is broken. The precise description of axially asymmetric shapes and the resulting triaxial quantum many-body rotors remains open questions in nuclear physics and, since they are also being developed for other finite quantum systems like polyatomic molecules [2], presents a topic of broad interest.

Quadrupole shape deformations can be described in terms of the polar deformation parameters  $\beta$  and  $\gamma$  [1]. The parameter  $\beta$  is proportional to the intrinsic quadrupole moment, and the angular variable  $\gamma$  specifies the type of the shape. The limit  $\gamma = 0$  corresponds to axial prolate shapes, whereas the shape is oblate for  $\gamma = \pi/3$ . Triaxial shapes are associated with intermediate values  $0 < \gamma < \pi/3$ . The latter have been investigated extensively using theoretical approaches that are essentially based on the rigid-triaxial rotor model of Davydov and Filippov [3], and the  $\gamma$ -unstable rotor model of Wilets and Jean [4]. The former assumes that the collective potential has a stable minimum at a particular value of  $\gamma$ , whereas in the latter the potential is independent of  $\gamma$  and thus the corresponding collective wave functions are extended in the  $\gamma$  direction.

However, presumably all known axially-asymmetric nuclei exhibit features that are almost exactly in between these two geometrical limits, characterized by the energy-level pattern of quasi- $\gamma$  band: relative locations of the odd-spin to the even-spin levels. As the two models originate from different physical pictures, the question of whether axially-asymmetric nuclei are  $\gamma$  rigid or unstable has attracted considerable theoretical interest

[1, 5–7]. The present Letter addresses this question from a microscopic perspective, and identifies the appropriate Hamiltonian of the interacting boson model (IBM) [5] for  $\gamma$ -soft nuclei, consistent with the microscopic picture. We thereby provide a solution to the problem concerning the energy-level pattern of the odd-spin states.

At present the most complete microscopic description of ground-state properties and collective excitations over the whole chart of nuclides is provided by the framework of energy density functionals (EDFs). Both non-relativistic [8–11], and relativistic [12, 13] EDFs have successfully been employed in numerous studies of shape phenomena and the resulting complex excitation spectra and decay patterns [14–17]. The starting point is usually a constrained self-consistent mean-field calculation of the energy surface with the mass quadrupole moments as constrained quantities [6]. This is illustrated in the first row of Fig. 1, where we display the self-consistent quadrupole energy surfaces of  $^{134}\text{Ba}$  (a) and  $^{190}\text{Os}$  (b) in the  $\beta - \gamma$  plane. The constrained energy surface of  $^{134}\text{Ba}$  is calculated using the relativistic Hartree-Bogoliubov model [12] with the DD-PC1 [18] functional, and that of  $^{190}\text{Os}$  employing the Hartree-Fock plus BCS model [19] with the Skyrme functional SkM\* [20]. These functionals are representative of the two classes – relativistic and non-relativistic EDFs, and will be used throughout this work to demonstrate that the principal conclusions do not depend on the particular choice of the EDF. One notices in Figs. 1(a) and 1(b) that in both cases the energy surface is very soft in  $\gamma$ , with  $^{134}\text{Ba}$  displaying a nearly  $\gamma$ -independent picture, whereas a more pronounced rigid triaxial shape is predicted for  $^{190}\text{Os}$  with the minimum at  $\gamma \approx 30^\circ$ .

To calculate excitation spectra and transition rates, it is necessary to go beyond the mean-field solution and explicitly take into account collective correlations. Here we employ the IBM to analyze spectroscopic properties of  $\gamma$ -soft nuclei. The O(6) dynamical symmetry [5] of

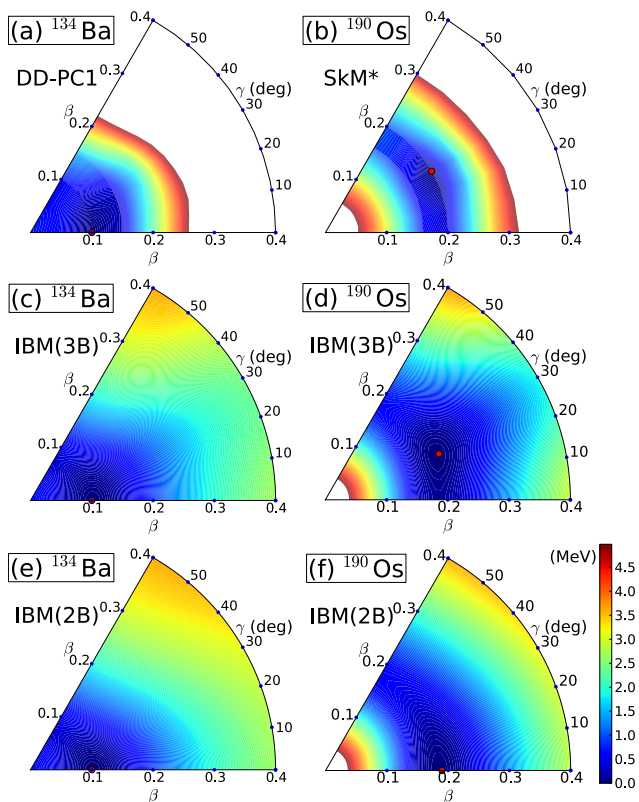


FIG. 1. (Color online) Self-consistent energy surfaces of  $^{134}\text{Ba}$  (a) and  $^{190}\text{Os}$  (b) up to 5 MeV in energy from the minima with the DD-PC1 and with the Skyrme SkM\* functionals, respectively. The corresponding mapped energy surfaces of the IBM with (middle row) and without (lower row) the three-body term of Eq. (2) are plotted.

IBM presents a good approximation to a system with  $\gamma$ -independent collective potential. The geometrical picture of the  $O(6)$  limit of the IBM emerges in the coherent-state framework [21], being consistent with the model of Wilets and Jean [4]. The coherent state represents the intrinsic wave function of the boson system, and  $O(6)$  states in the laboratory system can be generated by angular momentum projection [21]. The triaxial-rotor features of the IBM were emphasized already in [22, 23], leading to the “equivalence” ansatz of the  $\gamma$ -rigid and the  $O(6)$  descriptions of the low-lying spectra [24].

The present study uses the proton-neutron IBM (IBM-2), which includes proton (neutron) monopole  $s_\pi$  ( $s_\nu$ ) and quadrupole  $d_\pi$  ( $d_\nu$ ) bosons, representing  $J^\pi = 0^+$  and  $2^+$  collective pairs of valence protons (neutrons), respectively [25]. The number  $N_\pi$  ( $N_\nu$ ) of proton (neutron) bosons equals the number of valence proton (neutron) pairs (particles or holes), with respect to the nearest proton (neutron) closed shell [25]. The following IBM-2 Hamiltonian is employed:

$$H_{\text{IBM}} = \epsilon(n_{d\pi} + n_{d\nu}) + \kappa Q_\pi \cdot Q_\nu + H_{3\text{B}} \quad (1)$$

with the  $d$ -boson number operator  $n_{d\rho} = d_\rho^\dagger \cdot \tilde{d}_\rho$  ( $\rho =$

$\pi, \nu$ ), and the quadrupole operator  $Q_\rho = s_\rho^\dagger \tilde{d}_\rho + d_\rho^\dagger s_\rho + \chi_\rho [d_\rho^\dagger \tilde{d}_\rho]^{(2)}$ . The third term  $H_{3\text{B}}$  on the right-hand side of Eq. (1) denotes the three-body boson interaction:

$$H_{3\text{B}} = \sum_{\rho \neq \rho'} \sum_L \theta_L^\rho [d_\rho^\dagger d_\rho^\dagger d_{\rho'}^\dagger]^{(L)} \cdot [\tilde{d}_{\rho'} \tilde{d}_\rho \tilde{d}_\rho]^{(L)}. \quad (2)$$

The three-body term was introduced and analyzed in the IBM-1 framework (without distinction between proton and neutron bosons) [26, 27], but is used here for the first time in the microscopic IBM-2 model. In the IBM-2 there could be three-body terms with combinations of proton and neutron  $d$ -boson operators different from the one used in Eq. (2). However, since the proton-neutron quadrupole interaction dominates over the proton-proton and neutron-neutron ones for medium-heavy and heavy deformed nuclei, the term (2) represents the dominant contribution of three-body boson interactions. For each  $\rho$  and  $\rho'$ , there are five linearly independent combinations in Eq. (2), determined by the value of  $L = 0, 2, 3, 4, 6$  [26]. However, only the term with  $L = 3$  can give rise to a stable triaxial minimum at  $\gamma \approx 30^\circ$  [27], because its expectation value in the classical limit is proportional to  $\cos^2 3\gamma$ . We thus consider only the  $L = 3$  in Eq. (2) and, in addition, assume  $\theta_3^\pi = \theta_3^\nu \equiv \theta_3$ .

The parameters  $\epsilon$ ,  $\kappa$ ,  $\chi_{\pi,\nu}$  and  $\theta_3$  are adjusted following the procedure of Ref. [14]: the microscopic quadrupole energy surface, obtained from a mean-field calculation using a given EDF, is mapped onto the corresponding boson energy surface, i.e., expectation value of  $H_{\text{IBM}}$  in the coherent state (cf. [14, 28] for details). The deduced value of  $\theta_3 > 0$  varies gradually with boson number:  $|\theta_3/\kappa| \approx 1$  for  $1 \leq N_\pi + N_\nu \lesssim 5$  and  $\approx 0.5$  for  $5 \lesssim N_\pi + N_\nu \leq 10$ .

Without three-body boson terms the energy expectation value either has a minimum at  $\gamma = 0^\circ$  (prolate shapes) or  $60^\circ$  (oblate shapes), or is independent of  $\gamma$  in the  $O(6)$  limit. Triaxial minima are obtained only after the inclusion of the three-body interaction  $H_{3\text{B}}$ . This is nicely illustrated in Fig. 1, where the mapped energy surfaces of the IBM are plotted in the middle row (for the full IBM Hamiltonian Eq. (1) that contains the three-body term), and in the lower row (for the IBM Hamiltonian without the three-body term). For  $^{190}\text{Os}$  the Hartree-Fock plus BCS model with the Skyrme functional SkM\* predicts a minimum at  $\gamma \approx 30^\circ$ , which can only be reproduced on the mapped surface corresponding to the expectation value of the full IBM Hamiltonian containing the three-body term (Fig. 1(d)). The contribution of this term to the mapped energy surface is in general less important when the number of active bosons becomes relatively small. Thus for  $^{134}\text{Ba}$  nucleus in Fig. 1(c) the minimum is still on prolate axis even when the three-body term is included. The IBM Hamiltonian with up to two-body terms yields an energy surface that is soft in the  $\gamma$  degree of freedom (cf. Fig. 1(f)), but the minimum is on the  $\gamma = 0^\circ$  axis. We note that while the angular variables  $\gamma$  of the boson energy surface and the constrained microscopic energy surface are identical to each other, the axial deformation parameters  $\beta$  are related by

a constant of proportionality determined by equating the corresponding intrinsic quadrupole moments [14]. The geometrical variable  $\beta$  is obtained by multiplying the boson axial deformation by factors  $\approx 0.15$  and  $0.2$  for  $^{134}\text{Ba}$  and  $^{190}\text{Os}$ , respectively.

A distinction between  $\gamma$ -unstable and rigid-triaxial nuclei arises when considering the ratio of excitation energies [7]:  $S(J, J-1, J-2) \equiv [\{E(J) - E(J-1)\} - \{E(J-1) - E(J-2)\}]/E(2_1^+)$  for the quasi- $\gamma$  ( $K^\pi = 2^+$ ) band  $J^\pi = 2_\gamma^+, 3_\gamma^+, 4_\gamma^+ \dots$ , etc. The excitation energies  $E(J)$  are obtained by diagonalization of the Hamiltonian  $H_{\text{IBM}}$ , and the quadrupole operators  $Q_\rho$  are used in the calculation of E2 transition rates, with identical proton and neutron boson effective charges.

For a characteristic set of non-axial medium-heavy and heavy nuclei, in Fig. 2 we plot the energy ratios  $S(4, 3, 2)$  (a) and  $S(5, 4, 3)$  (b), as functions of the product of proton and neutron boson numbers:  $N_\pi N_\nu$ . The latter quantity reflects the amount of valence proton-neutron correlations, and hence the increase of  $N_\pi N_\nu$  corresponds to an enhancement of collectivity [7]. In this work we consider non-axial nuclei in the mass regions  $A \sim 110, 130$  and  $190$ , whose spectra display signatures of  $\gamma$ -softness. The set of nuclei shown in Fig. 2 has been selected so that the corresponding values of  $N_\pi N_\nu$  evenly span the widest possible range. The IBM excitation spectra have been calculated starting from self-consistent mean-field energy surfaces that correspond to the two functionals, Skyrme SkM\* and the relativistic DD-PC1. The two energy ratios, calculated with and without the three-body term of Eq. (2) in the IBM Hamiltonian, are plotted in comparison to data [29], and the predictions of the rigid-triaxial rotor model of Davydov and Filippov [3] and the  $\gamma$ -unstable rotor model of Wilets and Jean [4]. One notices that for all considered nuclei data can only be reproduced with the IBM Hamiltonian that includes the three-body term Eq. (2). Both the empirical and calculated ratios fall almost exactly in between the limits of the  $\gamma$ -unstable rotor and the rigid-triaxial rotor models: the Wilets-Jean limit is  $-2.00$  and the Davydov-Filippov limit is  $1.67$  for  $S(4, 3, 2)$ ; the Wilets-Jean model predicts  $2.50$ , and Davydov-Filippov  $-2.33$  for  $S(5, 4, 3)$ . The IBM Hamiltonian with up to two-body terms cannot reproduce the empirical values and, in both cases, yields energy ratios that are close to the predictions of the  $\gamma$ -unstable rotor model.

While the energy ratios are largely independent of the product of boson numbers, the  $B(E2)$  systematics reflects the evolution of collectivity. For instance, the ratio  $B(E2; 3_1^+ \rightarrow 2_2^+)/B(E2; 2_1^+ \rightarrow 0_1^+)$ , plotted in Fig. 2(c), gradually increases with  $N_\pi N_\nu$ . For nuclei with typically low  $N_\pi N_\nu$  ( $\leq 10$ ), like  $^{132,134}\text{Ba}$  and  $^{194,196}\text{Pt}$ , the  $\gamma$  value on average is close to  $0^\circ$  or  $60^\circ$ . In this case the ratio  $B(E2; 3_1^+ \rightarrow 2_2^+)/B(E2; 2_1^+ \rightarrow 0_1^+)$  is closer to the Wilets-Jean limit ( $O(6)$  in the IBM representation) of  $1.19$ . As the collectivity evolves with  $N_\pi N_\nu \geq 12$ , this  $B(E2)$  ratio, calculated with the full IBM Hamiltonian that includes the three-body term, saturates be-

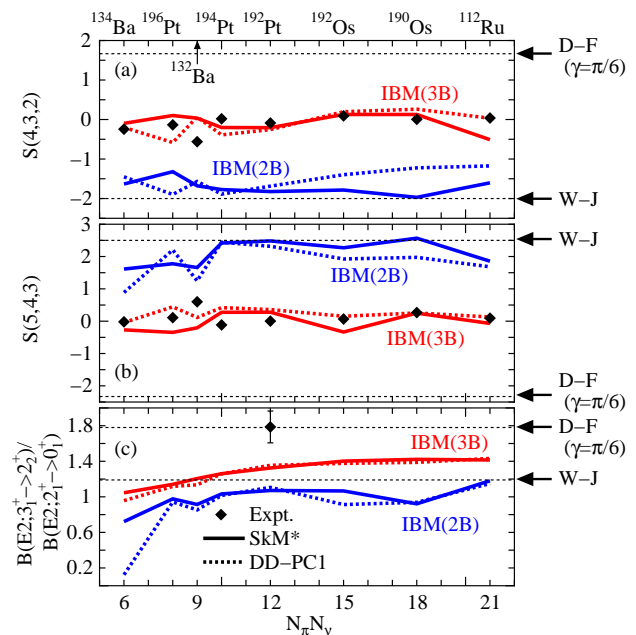


FIG. 2. (Color online) The energy ratios (a)  $S(4, 3, 2)$  and (b)  $S(5, 4, 3)$ , and (c) the  $B(E2; 3_1^+ \rightarrow 2_2^+)/B(E2; 2_1^+ \rightarrow 0_1^+)$  ratio, as functions of the product  $N_\pi N_\nu$ , for a characteristic set of non-axial medium and heavy nuclei. IBM(3B) and IBM(2B) denote results obtained with the IBM Hamiltonians with up to three- and two-body terms, respectively. The Skyrme SkM\* and relativistic DD-PC1 functionals are used. Data are from Refs. [29, 30], and D-F and W-J denote the limits of the rigid-triaxial and the  $\gamma$ -unstable (or  $O(6)$ ) models, respectively.

tween the  $\gamma$ -rigid limit of  $1.78$  and the  $\gamma$ -unstable limit of  $1.19$ , in agreement with behavior of the energy ratios  $S(J, J-1, J-2)$ . The  $B(E2)$  ratio calculated with the IBM Hamiltonian with up to two-body terms remains close to the  $O(6)$  limit even for large values of  $N_\pi N_\nu$ .

Although the ratios shown in Fig. 2 are calculated using two completely different microscopic density functionals, it appears that the basic features of this analysis are not sensitive to the particular choice of the underlying EDF.

In the IBM picture, the number of proton (neutron) bosons equals half the number of the corresponding valence particles or holes [25]. Among the nuclei discussed in this Letter, those with relatively large  $N_\pi N_\nu$  ( $\geq 12$ ), in many of which both  $N_\pi$  and  $N_\nu$  correspond to hole configurations, are more likely to exhibit pronounced  $\gamma$  rigidity, compared to systems with low  $N_\pi N_\nu$  ( $\leq 10$ ). In most of the latter cases  $N_\pi$  ( $N_\nu$ ) corresponds to particle (hole) configuration, or vice versa.

The discussion so far has focused on the systematics of energy ratios and transition rates. The model, however, provides an equally accurate and complete description of low-energy excitation spectra in individual nuclei. This is highlighted by the level scheme of  $^{190}\text{Os}$  in Fig. 3. Again we compare results obtained with IBM Hamiltonians con-

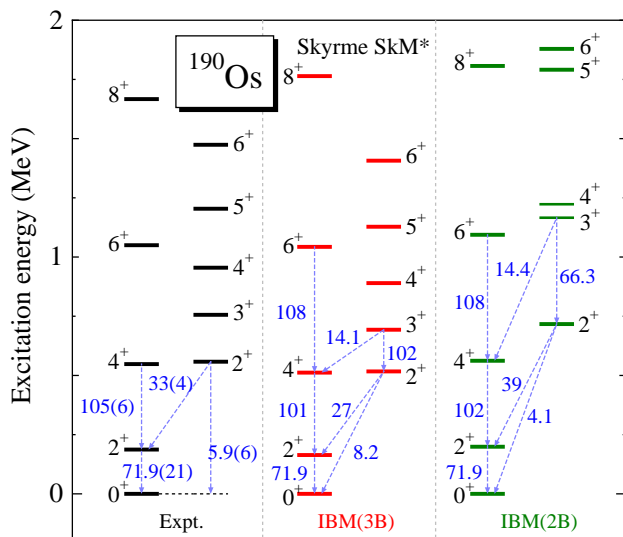


FIG. 3. (Color online) Low-lying spectra and  $B(E2)$  values (in Weisskopf units) of  $^{190}\text{Os}$ . The bands calculated with IBM Hamiltonians with (IBM(3B)) and without (IBM(2B)) the three-body term of Eq. (2) are compared to experimental data [31]. The Skyrme SkM\* EDF is used, and the boson effective charge is adjusted to reproduce the experimental value of  $B(E2; 2_1^+ \rightarrow 0_1^+)$ .

taining up to two- and three-body terms to available data [29, 31]. The full IBM Hamiltonian  $H_{\text{IBM}}$  reproduces both the excitation energies and transition rates for the ground-state band and the band built on the state  $2_2^+$  (quasi- $\gamma$  band). We notice the marked effect of the three-body term on the quasi- $\gamma$  band: all states are lowered in energy but, in particular, the pronounced lowering of the odd-spin states, e.g.,  $3_1^+$  and  $5_1^+$  by 473 keV and 663 keV,

respectively, breaks the quasi-degeneracy of the doublets ( $3_1^+, 4_2^+$ ), ( $5_1^+, 6_2^+$ ), etc [32]. These doublets ( $\tau$ -multiplets) are characteristic of the  $\gamma$ -unstable O(6) limit of IBM [5]. We emphasize that there are no additional adjustable parameters in the calculation of excitation energies, that is, the parameters are completely determined by the choice of the microscopic functional and the mapping procedure. Results of similar level of agreement with experiment are also obtained in the calculation of spectra of other nuclei considered in this study.

In conclusion, we have investigated the emergence of  $\gamma$  softness in atomic nuclei starting from the microscopic framework of energy density functionals. For a wide range of relevant nuclei certain observables allow us, in comparison to microscopic calculations, to differentiate two limiting geometrical pictures: the rigid-triaxial and the  $\gamma$ -unstable rotors. The present analysis clearly demonstrates that neither of these pictures is realized in actual nuclei. Typical non-axial medium-heavy and heavy nuclei lie almost exactly in the middle between the two geometrical limits, as a robust regularity. In the IBM framework the regularity arises naturally only when a three-body boson interaction is included. This result points to the origin of the three-body boson interaction, suggesting the optimal IBM description of  $\gamma$ -soft nuclei. The principal results presented in this Letter do not depend on details of the EDF, and suggest us a comprehensive picture of triaxial shapes of atomic nuclei in a fully microscopic way, including a solution to the long-standing problem of the energy-level pattern of odd-spin states.

This work has been supported in part by grants-in-aid for Scientific Research (A) 20244022 and No. 217368, and by MZOS - project 1191005-1010. K.N. and D.V. acknowledge support by the JSPS. T.N. acknowledges support by the Croatian Science Foundation.

- 
- [1] A. Bohr and B. R. Mottelson, *Nuclear Structure*, (Benjamin, New York, 1969 and 1975), Vols. I and II.
- [2] G. Herzberg, *Molecular spectra and molecular structure*, (Van Nostrand, New York, 1945), Vol. II.
- [3] A. S. Davydov and G. F. Filippov, Nucl. Phys. **8**, 237 (1958).
- [4] L. Wilets and M. Jean, Phys. Rev. **102**, 788 (1956).
- [5] F. Iachello and A. Arima, *The Interacting boson model* (Cambridge University Press, Cambridge, 1987).
- [6] P. Ring and P. Schuck, *The Nuclear Many-Body Problem* (Springer, Berlin, 1980).
- [7] R. F. Casten, *Nuclear Structure from a Simple Perspective*, (Oxford University Press, 1990, Oxford, UK).
- [8] M. Bender *et al.*, Rev. Mod. Phys. **75**, 121 (2003).
- [9] J. Erler, P. Klüpfel, and P.-G. Reinhard, J. Phys. G: Nucl. Part. Phys. **38**, 033101 (2011).
- [10] T. H. R. Skyrme, Nucl. Phys. **9**, 615 (1959) ; D. Vautherin and D. M. Brink, Phys. Rev. C **5**, 626 (1972).
- [11] J. Decharge *et al.*, Phys. Lett. B **55**, 361 (1975).
- [12] D. Vretenar *et al.*, Phys. Rep. **409**, 101 (2005).
- [13] T. Nikšić, D. Vretenar, and P. Ring, Prog. Part. Nucl. Phys. **66**, 519 (2011).
- [14] K. Nomura, N. Shimizu, and T. Otsuka, Phys. Rev. Lett. **101**, 142501 (2008).
- [15] M. Bender and P.-H. Heenen, Phys. Rev. C **78**, 024309 (2008).
- [16] T. R. Rodríguez and J. L. Egido, Phys. Rev. C **81**, 064323 (2010).
- [17] T. Nikšić, D. Vretenar, G. A. Lalazissis, and P. Ring, Phys. Rev. Lett. **99**, 092502 (2007).
- [18] T. Nikšić, D. Vretenar, and P. Ring, Phys. Rev. C **78**, 034318 (2008).
- [19] P. Bonche *et al.*, Comput. Phys. Comm. **171**, 49 (2005).
- [20] J. Bartel *et al.*, Nucl. Phys. **A386**, 79 (1982).
- [21] J. N. Ginocchio and M. W. Kirson, Nucl. Phys. A **350**, 31 (1980).
- [22] R. F. Casten *et al.*, Phys. Rev. C **29**, 356 (1984).
- [23] O. Castaños *et al.*, Phys. Rev. Lett. **52**, 263 (1984).
- [24] T. Otsuka and M. Sugita, Phys. Rev. Lett. **59**, 1541 (1987).

- [25] T. Otsuka *et al.*, Nucl. Phys. A **309** 1 (1978).
- [26] P. Van Isacker and J.-Q. Chen, Phys. Rev. C **24**, 684 (1981).
- [27] K. Heyde *et al.*, Phys. Rev. C **29**, 1420 (1984).
- [28] K. Nomura, N. Shimizu, and T. Otsuka, Phys. Rev. C **81**, 044307 (2010).
- [29] NuDat 2.5 [<http://www.nndc.bnl.gov/nudat2/index.jsp>].
- [30] C. M. Baglin, Nuclear Data Sheets **84**, 717 (1998).
- [31] B. Singh, Nuclear Data Sheets **99**, 275 (2003).
- [32] The lowest  $3^+$  level is predicted too high in many IBM calculations for  $\gamma$ -soft nuclei, and the empirical lowering was often ascribed to a possible coupling to two-quasiparticle states. The present work suggests that such a mechanism could play only a minor role.